## CHAPTER 185

# MODELING OF WAVE-CURRENT INTERACTION AND BEACH CHANGE

## Susumu OHNAKA\* and Akira WATANABE\*\*

### ABSTRACT

This paper presents a mathematical model of waves, currents and beach change with wave-current interaction. The wave model is based on the time-dependent mild-slope equations extended to a wave-current coexisting field, and is applicable to the computation of wave deformation due to combined effects of shoaling, refraction, diffraction, reflection, breaking and currents. Some examples of numerical computation are shown, and effects of the wave-current interaction on the nearshore waves, currents and beach evolution is discussed. In addition, a simple treatment of obliquely incident wave condition as well as improvement of sediment transport rate formulas are presented.

### 1 INTRODUCTION

Not a few mathematical models of nearshore processes have recently been developed and applied to the prediction of nearshore waves, currents and beach evolution. In most models, however, effects of the interaction between waves and currents are neglected. In actuality nearshore waves induce currents through radiation stresses, and resultant currents conversely affect the wave field; namely, the wave-current interaction always takes place to a greater or less extent. Under certain conditions, it will become very important to take the interaction effects into consideration for an accurate prediction of nearshore waves and currents as well as resultant sediment

<sup>\*</sup> Research Engineer, Technical Research Institute, Toa Corporation, 1-3, Anzencho, Tsurumi-ku, Yokohama, 230 Japan

<sup>\*\*</sup> Professor, Department of Civil Engineering, Univ. of Tokyo, Hongo-7, Bunkyo-ku, Tokyo, 113 Japan

transport and beach change.

In order to incorporate the wave-current interaction into nearshore process models, the wave deformation due to currents should be included in the computation of waves. For a wave field coexisting with a varying current in the water of non-uniform depth, a few kinds of wave models have been proposed (Booij, 1981; Liu, 1983; Kirby, 1984). These models are based on elliptic-type partial differential equations, which are in general rather difficult to solve numerically. Hence these equations are sometimes approximated by parabolic equations, but then they become inapplicable to a wave field including significant reflection from structures. On the other hand, Ohnaka et al. (1988) have proposed another kind of numerical computation model for a nearshore wave field with a varving current and depth. Their model employs time-dependent mildslope equations, and is applicable to the computation of wave deformation due to combined effects of shoaling. refraction, diffraction, reflection and breaking as well as wave-current interaction.

In the present study, this wave model is utilized as a part of a mathematical model of nearshore processes, and the effects of the wave-current interaction on the nearshore waves, currents and beach change are discussed on the basis of the results of numerical computation for two typical cases. Treatment of obliquely incident waves and improvement of sediment transport formulas are also presented.

## 2. BASIC EQUATIONS AND METHODS IN THE MODEL

### 2.1 Wave Computation

Ohnaka et al. (1988) have proposed time-dependent mild-slope equations for a wave-current coexisting field, which are applicable to the computation of wave deformation due to combined effects of the shoaling, refraction, diffraction, reflection and breaking as well as the wave-current interaction. The equations have been derived by separating the mild-slope equation for waves coexisting with a current proposed by Kirby (1984) into the following two equations expresses in terms of the water surface elevation ( and the depth-integrated flow rate vector Q:

$$\mathbf{m} \cdot (\partial \zeta / \partial t) + \nabla \cdot (\mathbf{U} \zeta) + \nabla \cdot (\mathbf{n} \mathbf{Q}) = 0 \tag{1}$$

$$\partial \mathbb{Q}/\partial t + \omega \mathbb{C}^{2} \nabla (\zeta/\sigma) + f_{D} \mathbb{Q} = 0$$
 (2)

$$m = 1 + (\sigma/\omega)(n-1), \qquad n = \mathbb{C}_{s}/\mathbb{C}$$
 (3).

where t is the time,  $\nabla$  is the horizontal gradient operator,  $\mathbb C$  and  $\mathbb C$ g are the phase and group velocity vectors and  $\mathbb U$  is the ambient current velocity vector. The last term in Eq. (2) is the energy dissipation term, where  $f_D$  is the energy dissipation coefficient to be defined later; this term has been added in order to deal with the wave decay and recovery after breaking. The apparent angular frequency  $\omega$  is defined by the following dispersion relation for a wave-current coexisting field:

$$\omega = \sigma + \mathbb{k} \cdot \mathbb{U}, \qquad \sigma = g \text{ k tanh k h}$$

where  $\sigma$  is the intrinsic angular frequency,  $\mathbb K$  is the wave number vector, h is the water depth, and g is the acceleration due to gravity. If the ambient current velocity vector  $\mathbb U$  is set to be zero, Eqs. (1) and (2) reduce to the original time-dependent mild-slope equations proposed by Watanabe and Maruyama (1986).

We need a value of the wave angle at every point to solve the above dispersion relation, Eq. (4). Since this wave model is based on the time-dependent equations, we can calculate the wave angle from values of  $\zeta$  and Q which have already been computed in the previous cycle over one wave period.

To determine the location of wave breaking, we adopted the breaker index for compound waves proposed by Watanabe et al. (1984), which is given by the ratio of the orbital velocity at the wave crest to the phase velocity as a function of the deepwater wave steepness and the local bottom slope. This breaker index will be applicable to the wave-current coexisting field by using values relative to the current for both the orbital velocity and the phase velocity.

As for the energy dissipation coefficient f<sub>D</sub>, Eq. (5) proposed by Watanabe and Dibajnia (1988), which can express not only the wave decay but also the wave recovery in the surf zone.

$$f_{D} = \alpha_{D} \tan \beta \sqrt{\frac{g}{h}} \sqrt{\frac{Q_{m} - Q_{r}}{Q_{r} - Q_{s}}}$$
 (5)

where  $\tan \beta$  is a representative bottom slope around a breaking point,  $\alpha_D$  is a nondimensional coefficient whose value is 2.5,  $Q_m$  is the amplitude of  $Q_n$ ,  $Q_n$  is the flow rate amplitude of breaking waves on a uniform slope, and  $Q_n$  is that of recovering waves in a constant depth region. The quantities  $Q_n$  and  $Q_n$  are expressed as

$$Q_s = \gamma_s c n, \quad Q_r = \gamma_r c h \tag{6}$$

According to experimental data, the coefficients  $\gamma_S$  and  $\gamma_r$  are given by

$$\gamma_s = 0.4(0.57 + 5.3 \tan \beta), \qquad \gamma_r = 0.4(a/h)_b$$
 (7)

where  $(a/h)_b$  is the ratio of the wave amplitude to the water depth at a breaking point.

It has been demonstrated by Ohnaka et al. (1988) that the above breaker index and the energy dissipation factor are applicable to the computation of cross-shore distribution of wave height in a wave-current coexisting field with sufficient accuracy.

# 2.2 Current Computation

The current field is calculated by commonly used depth-average equations of the mean flow as follows:

$$\frac{\partial \overline{\zeta}}{\partial t} + \frac{\partial U(h + \overline{\zeta})}{\partial x} + \frac{\partial V(h + \overline{\zeta})}{\partial y} = 0$$
 (8)

$$\frac{\partial U}{\partial t} + U \frac{\partial U}{\partial x} + V \frac{\partial U}{\partial y} + g \frac{\partial \overline{\zeta}}{\partial x} + Rx + Fx - Mx = 0$$
 (9)

$$\frac{\partial V}{\partial t} + U \frac{\partial V}{\partial x} + V \frac{\partial V}{\partial y} + g \frac{\partial \overline{\zeta}}{\partial y} + Ry + Fy - My = 0$$
 (10)

where  $(x,\ y)$  are Cartesian coordinates in a horizontal plane,  $(U,\ V)$  are the corresponding velocity components of the mean flow,  $\overline{\zeta}$  is the elevation of the mean water surface measured from the still water level,  $(R_X,\ R_y)$  are the radiation stress terms,  $(F_X,\ F_y)$  are the bottom friction terms, and  $(M_X,\ M_y)$  are the lateral mixing terms.

In order to treat the wave-current interaction, alternate computations of waves and of currents are necessary. An efficient iteration scheme is required so as to obtain the convergence of solutions in a computation time as short as possible. For this, no-current condition is assumed in the first step of wave computation as shown in Fig. 1. Then reduced values of radiation stresses  $R_1$  are used in the first cycle of current computation, because if the actual values of radiation stresses  $R_1$  calculated from the wave solutions are adopted, a large number of iterations are required to attain the convergence. Waves in the next step are calculated using the resultant reduced current velocity  $U_1$ . The reduction rate of radiation stresses is

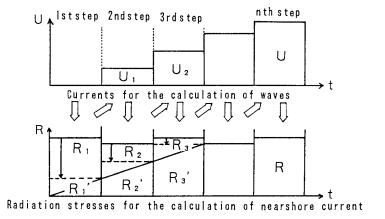


Fig. 1 Iteration of computations for waves and currents.

gradually decreased for every step, and finally full values of the radiation stresses and resultant currents are adopted for the calculation of currents and of waves, respectively.

# 2.3 IMPROVEMENT OF FORMULAS FOR SEDIMENT TRANSPORT RATES

Watanabe et al. (1986) proposed formulas for sediment transport rates under combined action of waves and currents on the basis of the power model concept. In their formulas the sediment transport rates are treated as summation of those due to waves  $q_W$  and due to currents  $q_C$ , which are expressed, respectively, by

$$q_{\mathsf{w}} = A_{\mathsf{w}}(\tau_{\mathsf{h}} - \tau_{\mathsf{cr}}) F \widehat{\mathsf{u}}_{\mathsf{h}} / (\rho g)$$
 (11)

$$\mathbf{q_c} = \mathbf{A_c} (\tau_b - \tau_{cr}) \, \mathbb{U} / (\rho \, \mathbf{g}) \tag{12}$$

where  $A_W$  and  $A_C$  are nondimensional coefficients, values of which should be empirically determined,  $\tau_b$  is the maximum value of the bottom shear stress in a wavecurrent coexisting system,  $\tau_{CT}$  is the critical shear stress for the onset of general movement of sediment grains,  $\hat{U}_b$  is the amplitude of the near-bottom wave orbital velocity vector,  $\rho$  is the density of water, and  $F_D$  is the net transport direction function. The bottom shear stress  $\tau_b$  for a wave-current coexisting system is evaluated by the friction law proposed by Tanaka and Shuto (1981). Since this friction law is based on the bottom boundary layer theory, its applicability to the surf zone, where turbulence due to wave breaking is

predominant, is questio...able. In the present model, therefore, the effects of the breaker-induced turbulence are incorporated in addition to the bottom shear stress as sediment-entraining forces in the surf zone. Namely the improved formulas for sediment transport rates are expressed as follows:

$$q_{lw} = \{A_w(\tau_b - \tau_{cr}) + A_{wb}\tau_t\} F_D \widehat{u}_b/(\rho g)$$
 (13)

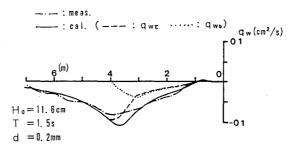
$$q_c = \{A_c(\tau_b - \tau_{cr}) + A_{cb}\tau_t\} \ U/(\rho g)$$
 (14)

where  $\tau_t$  is the breaker-induced turbulent stress, and  $A_{wb}$  and  $A_{cb}$  are nondimensional coefficients. The magnitude of  $\tau_t$  is evaluated from the rate of energy dissipation by the following formula based on a dimensional analysis and experimental data:

$$\tau_{t} = \rho^{1/3} (n f_{D} E)^{2/3}$$
 (15)

where  $nf_DE$  is the breaker-induced energy dissipation rate per unit area and time.

To examine the applicability of these formulas, numerical computation has been conducted for the cross-shore sediment transport rates on a beach with initially uniform slope of 1/20. Figure 2 shows the comparisons between the computation and measurements of cross-shore distributions of the transport rates. The upper figure is for the case of offshore transport, while the lower is for that of onshore transport. The dash-dot lines



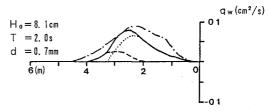


Fig. 2 Cross-shore distributions of transport rates.

show the measured transport rates and solid lines indicate the calculated ones. The component due to the bottom shear stress  $q_{WT}$  and that due to the breaker-induced stress  $q_{Wb}$  are shown by the dash and the dot lines, respectively. Computed transport rates agree fairly well with the measured ones.

The change in local bottom elevation,  $z_b$  is calculated from the spatial distribution of the sediment transport rates by solving the following equation for the conservation of sediment volume:

$$\frac{\partial z_b}{\partial t} = -\frac{\partial q_x}{\partial x} - \frac{\partial q_y}{\partial y}$$

$$q = q_w + q_c = (q_x, q_y)$$
(16)

where  $(q_X', q_y')$  are the components of the transport rates in the x- and y-directions corrected in order to include the bottom slope effect, and are given by

$$q_{x}' = q_{x} - \varepsilon_{s} \mid q_{x} \mid \frac{\partial z_{b}}{\partial t}$$
,  $q_{y}' = q_{y} - \varepsilon_{s} \mid q_{y} \mid \frac{\partial z_{b}}{\partial t}$  (17)

where  $\epsilon_{\text{S}}$  is the dimensionless coefficient of the order of unity.

### 3. NUMERICAL COMPUTATION METHOD FOR WAVES

Equations (1) and (2) are solved by using a finite difference method. For the discretization of the convection term due to mean flow in Eq. (1), the Alternating Direction Explicit (A. D. E.) scheme is adopted in order to solve explicitly without numerical diffusion as follows:

$$\left(\frac{\partial (U\zeta)}{\partial x}\right)_{\text{point=i}} = \frac{U_{i+1/2}\zeta_{i+1/2}^{j+1/2} - U_{i-1/2}\zeta_{i-1/2}^{j+1/2}}{\Delta x}$$

$$\zeta_{i+1/2}^{j+1/2} = 0.5(\zeta_{i}^{j} + \zeta_{i+1}^{j}), \quad \zeta_{i-1/2}^{j+1/2} = 0.5(\zeta_{i}^{j} + \zeta_{i-1}^{j+1})$$
(18)

Namely, as for  $\zeta$  at a point (i-1) which is needed for the discretization of the convection term at a point (i), its values at a time-step (j) are successively replaced with values at a time-step (j+1) calculated just before.

Now let us consider boundary conditions in the wave computation. The boundary conditions must be imposed on all the boundaries surrounding the computation region: namely, the offshore open boundary, shoreline boundary,

and two side boundaries.

Waves on the offshore open boundary are expressed as the superposition of the incident waves  $\zeta_I$  and the outgoing waves  $\zeta_R$  as shown in Eq. (19).

$$\zeta^{t}(x_{0}, y_{0}) = \zeta_{1}^{t}(x_{0}, y_{0}) + \zeta_{R}^{t}(x_{0}, y_{0})$$

$$\zeta_{1}^{t}(x_{0}, y_{0}) = a_{1}\sin(k x_{0}\cos\theta_{1} + k y_{0}\sin\theta_{1} - \sigma t)$$

$$\zeta_{R}^{t}(x_{0}, y_{0}) = \zeta^{t-\tau}(x_{0}, y_{0})$$

$$-a_{1}\sin\{(k (x_{0} + \Delta x)\cos\theta_{1} + k y_{0}\sin\theta_{1} - \sigma (t - \tau)\}\}$$
(19)

where  $a_I$  is the incident wave amplitude,  $\Delta x$  is the grid length normal to the boundary, and the subscript o denotes quantities at the boundary. The time shift  $\tau$  is defined by

$$\tau = \triangle x \cos \theta_{n} / C \tag{20}$$

where  $\theta_n$  is the direction angle of the outgoing wave component measured from the normal line to the boundary.

The shoreline is treated as a moving boundary to include the change in its location caused by the change in the mean water elevation due to wave setup, and  $\zeta$  is kept equal to 0 on this moving shoreline boundary.

In case of obliquely incident waves, one of the side boundaries becomes an incident boundary, while the other becomes an open boundary. For the open side boundary, the value of  $\zeta$  at a point  $(x_0, y_0)$  on the boundary at time t is set equal to the one at an adjacent inner point  $(x_0, y_0 - \Delta y)$  at time t- $\tau$  as follows:

$$\zeta^{t}(\mathbf{x}_{0}, \mathbf{y}_{0}) = \zeta^{t-\tau}(\mathbf{x}_{0}, \mathbf{y}_{0} - \triangle \mathbf{y})$$
(21)

The time shift au is defined by

$$\tau = \triangle y \sin \theta / (C + U \cos \theta + V \sin \theta)$$
 (22)

where  $\boldsymbol{\theta}$  is the wave direction angle measured from the x-axis.

On the other hand,  $\zeta$  on the incident side boundary is expressed as follows:

$$\zeta^{\prime}(x_0, y_0) = a(x_0)\sin\left(\int_0^{x_0} k\cos\theta \, dx + k\sin\theta \, y_0 - \sigma \, t\right) \tag{23}$$

In this equation, however, the wave amplitude  $a\left(x_{0}\right)$  is unknown because it changes towards the onshore direction owing to the shoaling, refraction, breaking, etc. The problem is how to determine  $a\left(x_{0}\right)$  along the boundary.

In the present study we propose a simple and practical computation method, in which the wave amplitude  $a\left(x_{0}\right)$  on the boundary is calculated from the quantities in the inner region by assuming the local wave periodicity in the alongshore direction. For this, an imaginary computation region is attached to the incident side boundary of the actual computation region as shown in Fig. 3. Assuming shore-parallel straight bottom contours in this region, we obtain Eq. (24).

$$L_{y} = L/\sin\theta = \text{const}. \tag{24}$$

where Ly is the wavelength in the alongshore direction. If the width of the imaginary region is set equal to Ly, waves change periodically in the alongshore direction, and consequently the following relation holds:

$$\zeta_{1,j} = \zeta_{Ny,j} \tag{25}$$

where  $\zeta_{1,j}$  is the water surface elevation on the lower boundary, and  $\zeta_{Ny,j}$  on the upper boundary of this imaginary region. Using this condition, we can calculate  $\zeta$  and Q in the imaginary region without specifying any values on the side boundaries.

Figures 4 and 5 are the results of numerical computation in imaginary regions for cases of constant depth and of uniform slope, respectively. Waves come into the region with an incident angle of 60 degrees. The width equal to Ly has been divided into 15 grids. The left and the right figures respectively show the distributions of the normalized wave height and of the phase. These results are quite satisfactory and indicate the validity of this treatment.

The values of  $\zeta_{Ny,j}$  thus obtained are given along the incident side boundaries in the computation for the actual region. Figure 6 is an example of the wave field computed for the case of obliquely incident waves. The

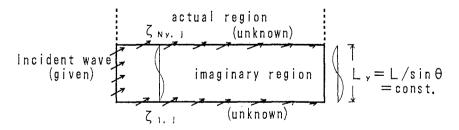


Fig. 3 Imaginary region.

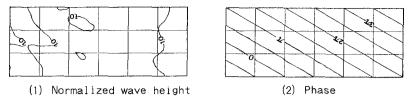


Fig. 4 Waves in the imaginary region for the case of constant depth.

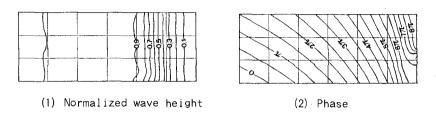
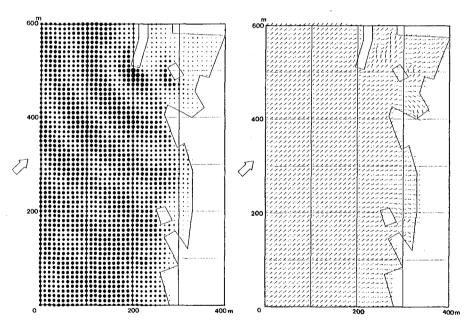


Fig. 5 Waves in the imaginary region for the case of uniform slope.



Distribution of wave height (2) Distribution of wave direction
 Fig. 6 Computed wave field for obliquely incident waves.

left and the right figures show the distributions of the wave height and the wave angle, respectively. As indicated in these results, incident waves come into theregion across not only the offshore boundary but also the lower side boundary.

# 4. EXAMPLES OF APPLICATION OF THE MODEL

The present numerical model has been applied to the computations of waves, currents and beach change for two typical cases involving the wave-current interaction.

The first case is for a region around detached breakwaters on a beach with initially uniform slope of 1/25. The incident wave height is 2.5 m, the period is and the incident direction is normal to the shoreline. It is difficult at the present stage to evaluate proper values of the coefficients in the sediment transport rate formulas because of insufficient experimental and field data. Values of  $A_{W}=0.15$ ,  $A_{C}=0.50$ ,  $A_{W}b=0.03$ , and  $A_{C}b=0.10$  has been adopted in this computation according to some experimental results. The grid size is  $\Delta x = \Delta y = 2.5$  m for the calculation of wave field and  $\Delta x = \Delta y = 5.0$  m for the calculation of nearshore current and beach change. Iteration in the calculation of waves and currents to include the wavecurrent interaction has been conducted nine times, and in the first four iteration steps values of the radiation stresses has been increased gradually by 25% for each step.

Figure 7 shows the wave height distribution, where the upper half gives the result computed with the wavecurrent interaction, and the lower half without the interaction. The differences of the wave height in the surf zone and of the breaker line are clearly observed. The distribution of the wave direction is shown in Fig. Refraction due to nearshore current is observed when the wave-current interaction is considered. The distribution of nearshore currents is presented in Fig. 9, where reduction of the current intensity due to interaction and the shoreline change induced by the wave setup are well recognized. The distribution of the mean water elevation is presented in Fig. 10. Significant wave setup variation near the shoreline without the wave-current iteration is smoothed out when the interaction is considered. Figure 11 is the resultant beach topography, in which significant effects of the wave-current interaction appear near the shoreline.

The second case is for a region around a rip channel as shown in Fig. 12. Figure 13 shows the normalized wave height distribution. The difference of the

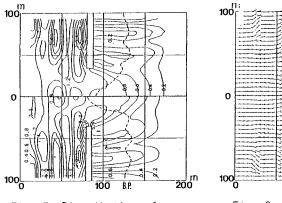


Fig. 7 Distribution of normalized wave height.

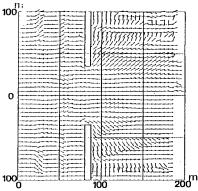


Fig. 8 Distribution of wave direction.

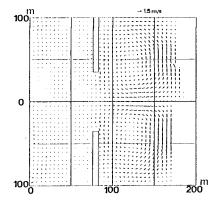


Fig. 9 Distribution of nearshore current.

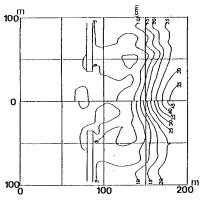


Fig. 10 Distribution of mean water elevation.

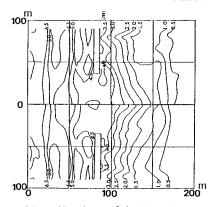
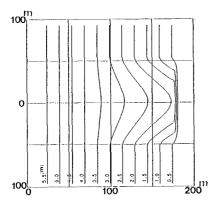


Fig. 11 Distribution of bottom topography.



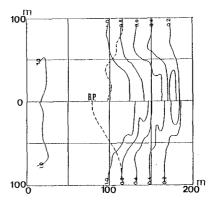
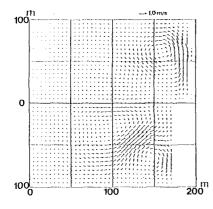


Fig. 12 Initial bottom topography around a rip channel.

Fig. 13 Distribution of normalized wave height.



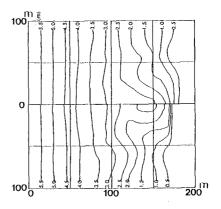


Fig. 14 Distribution of nearshore current.

Fig. 15 Distribution of Bottom topography.

breaker lines is clearly seen. The distribution of nearshore currents is presented in Fig. 14. The computation region is extended along the shoreline by the wave setup and in this expanded region a strong longshore current is observed. Rip current velocity is considerably reduced when the wave-current interaction is included. Figure 15 shows the resultant beach topography. In this case the sand transport due to waves has been ignored in order to emphasize the difference induced by the currents with and without the wave-current interaction. It is seen that the beach topography change is reduced when the wave-current interaction is considered.

### 5. CONCLUSIONS

A numerical computation model for nearshore waves, currents and beach change with wave-current interaction was presented, and the influences of the wave-current interaction were examined. It was shown that the wave-current interaction affected the wave field, current field and beach change in the nearshore zone. A treatment of the side boundary condition for the case of obliquely incident waves and improvement of sediment transport rate formulas were also presented, and their validity was demonstrated.

## REFERENCES

Booij, N. (1981): Gravity waves on water with non-uniform depth and current, Communications on Hydraulics, No. 81-1, Dept. of Civil Eng., Delft Univ. of Tech., 131p.

Kirby, J.T. (1984): A note on linear surface wavecurrent interaction over slowly varying topography, J. Geophy. Res., Vol. 89, No. C1, pp. 745-747.

Liu, P.L.F. (1983): Wave-current interaction on slowly varying topography, J. Geophys. Res., Vol. 88, No. C7, pp. 4421-4426.

Ohnaka, S and A Watanabe (1988): Numerical modeling of wave deformation with a current, Proc. 21st Coastal Eng. Conf., ASCE, pp. 393-407.

Tanaka, M and N Shuto (1981): Friction coefficient for a wave-current coexistent system, Coastal Eng. in Japan, Vol. 24, pp. 105-128.

Watanabe, A., T. Hara and K. Horikawa (1984): Study on breaking condition for compound wave trains, Coastal Eng. in Japan, Vol. 27, pp. 71-82.

Watanabe, A. and K. Maruyama (1986): Numerical modeling of nearshore wave field under combined refraction, diffraction and breaking, Coastal Eng. in Japan, Vol. 29, pp. 19-39.

Watanabe, A., K. Maruyama, T. Shimizu and T. Sakakiyama (1986): Numerical prediction model of three-dimensional beach deformation around a structure, Coastal Eng. in Japan, Vol. 29, pp. 179-194.

Watanabe, A. and M. Dibajnia (1988): A numerical model of wave deformation in surf zone, Proc. 21st Coastal Eng. Conf., ASCE, pp. 578-587.